Chemical Tuning of the Photon Upconversion Properties in Ti^{2+}-Doped Chloride Host Lattices

Oliver S. Wenger and Hans U. Güdel*

Departement für Chemie und Biochemie, Universität Bern, Freiestrasse 3, CH-3000 Bern 9, Switzerland

Received March 6, 2001

The photophysical properties of Ti^{2+}-doped NaCl and $MgCl_2$ at 15 K are compared. At this temperature both materials emit luminescence from their respective lowest excited states and from the $^3T_{1g}(t_{2g}e_g)$ higher excited state. In Ti^{2+}:$MgCl_2$ the ligand field is significantly stronger than in Ti^{2+}:NaCl, leading to $^1T_{2g}(t_{2g}^2)$ and $^3T_{2g}$-$(t_{2g}e_g)$ lowest excited states, respectively, in these materials. The near-infrared to visible upconversion mechanisms of these two materials are identified. The upconversion efficiency calculated for Ti^{2+}:$MgCl_2$ is approximately 2 orders of magnitude higher than for Ti^{2+}:NaCl. This is mainly due to the more efficient energy storage in the intermediate upconversion level in Ti^{2+}:$MgCl_2$, and its higher $^3T_{1g}(t_{2g}e_g) \rightarrow {}^3T_{1g}(t_{2g}^2)$ luminescence quantum yield relative to Ti^{2+}:NaCl.

I. Introduction

Aside from second-harmonic generation (SHG),[1] photon upconversion is a well-established and efficient method for the generation of short-wavelength radiation from long-wavelength pump sources.[2] In contrast to SHG, upconversion processes do not require coherent pump radiation. Thus upconversion materials have found use not only as solid-state laser materials[3] but also as phosphors.[4] A second fundamental difference between SHG and upconversion is the fact that the former process does not require any metastable excited states, whereas upconversion processes are restricted to systems with at least two metastable excited states. This basic prerequisite reduces the number of potential upconversion candidate systems very drastically, since it essentially demands a violation of Kasha's rule,[5] which states that typically only the lowest excited state of a given system will luminesce in the solid state. Exceptions to this rule are most commonly found among the rare earths, mainly among the trivalent lanthanides,[6] but also among the actinides.[7] This is due to the shielded nature of their spectroscopically active 4f and 5f electrons. Electron−phonon interaction, which determines the efficiency of nonradiative relaxation processes, is therefore relatively small in rare earth doped materials. Thus it is not surprising that the vast majority of photon upconversion materials known so far involve rare earth ions. However, the insensitivity of these ions to their chemical environment allows the experimentalist to take only relatively little control over their photophysical properties.

To date there exist comparatively few upconversion systems which are based on transition metal ions. Upconversion has previously been reported for octahedrally coordinated Ti^{2+},[8] Ni^{2+},[9,10] Mo^{3+},[11,12] Re^{4+},[11,13] and Os^{4+}.[14,15] Regarding upconversion properties, Ti^{2+} has so far received the smallest attention among these ions. Together with Ni^{2+}, Ti^{2+} is the only ion known to date which exhibits luminescence from a ligand field dependent higher excited state in octahedral coordination. An additional important difference between Ni^{2+} and Ti^{2+}, on the one hand, and the Mo^{3+}, Re^{4+}, and Os^{4+} ions, on the other hand, is the fact that in the former also the pump light absorption steps are ligand field dependent. From a chemist's point of view, Ni^{2+} and Ti^{2+} are thus very attractive upconversion ions, since they allow a goal-oriented modification of their upconversion properties by means of chemical variation. We have recently demonstrated a principle of environmental control of Ni^{2+} upconversion properties based on exchange interactions.[16,17]

In the present study we take advantage of the fact that the energy level sequence of Ti^{2+} is ligand field dependent: In weak ligand fields, i.e., at low values of 10 *Dq*, the first excited state is $^3T_{2g}(t_{2g}e_g)$, whereas in strong ligand fields, i.e., at high values of 10 *Dq*, it is a component of $^1T_{2g}(t_{2g}^2)$, see Figure 1. Thus, among all upconversion systems known to date, Ti^{2+}-doped systems offer the unique opportunity to control the identity of the first excited state, i.e., the intermediate state of the upconversion process, by chemical means. We have chosen Ti^{2+}:NaCl and Ti^{2+}:$MgCl_2$ as representative examples for weak and strong ligand field systems, respectively. Their individual ligand field strengths are indicated by the dashed vertical lines

(1) See, for example: Dalton, L. R.; Harper, A. W., Goshn, R.; Steier, W. H.; Ziari, M.; Fetterman, H.; Shi, Y.; Mustacich, R. V.; Jen, A. K.-Y.; Shea, K. J. *Chem. Mater.* **1995**, *7*, 1060−1081.
(2) Auzel, F. E. *Proc. IEEE* **1973**, *61*, 758−786.
(3) Lenth, W.; Macfarlane, R. M. *Opt. Photonics News* **1992**, *3*, 8−15.
(4) Downing, E.; Hesselink, L.; Ralston, J.; Macfarlane, R. *Science* **1996**, *273*, 1185−1189.
(5) Kasha, M. *Discuss. Faraday Soc.* **1950**, *9*, 14−19.
(6) Blasse, G.; Grabmaier, B. C. *Luminescent Materials*; Springer-Verlag: Berlin, 1994.
(7) Andres, H. P.; Krämer, K.; Güdel, H. U. *Phys. Rev. B* **1996**, *54*, 3830−3840.
(8) Jacobsen, S. M.; Güdel, H. U. *J. Lumin.* **1989**, *43*, 125−137.
(9) Oetliker, U.; Riley, M. J.; May, P. S.; Güdel, H. U. *Coord. Chem. Rev.* **1991**, *111*, 125−130 and references therein.
(10) Moncorge, R.; Benyattou, T. *Phys. Rev. B* **1988**, *37*, 9186−9196.
(11) Gamelin, D. R.; Güdel, H. U. *J. Am. Chem. Soc.* **1998**, *120*, 12143−12144.
(12) Gamelin, D. R.; Güdel, H. U. *J. Phys. Chem. B* **2000**, *104*, 10222−10234.
(13) Gamelin, D. R.; Güdel, H. U. *Inorg. Chem.* **1999**, *38*, 5154−5164.
(14) Wermuth, M.; Güdel, H. U. *Chem. Phys. Lett.* **1997**, *281*, 81−85.
(15) Wermuth, M.; Güdel, H. U. *J. Am. Chem. Soc.* **1999**, *121*, 10102−10111.
(16) Wenger, O. S.; Gamelin, D. R.; Güdel, H. U. *J. Am. Chem. Soc.* **2000**, *122*, 7408−7409.
(17) Wenger, O. S.; Güdel, H. U. *Inorg. Chem.* **2001**, *40*, 157−164.

10.1021/ic010255t CCC: $20.00
Published on Web 10/02/2001

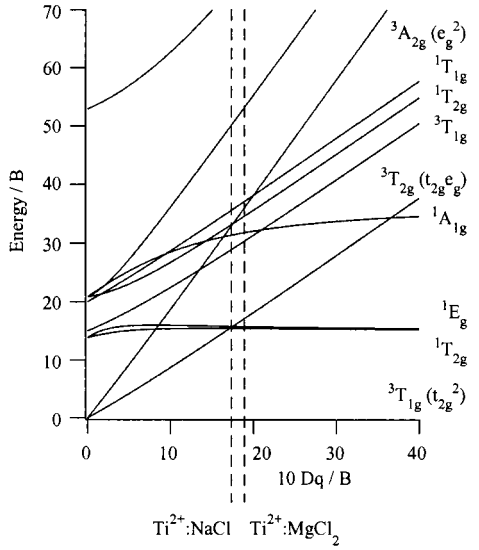

Figure 1. Energy level diagram for octahedrally coordinated d^2 ions. The dashed vertical lines indicate the positions of Ti^{2+} doped into NaCl and $MgCl_2$, respectively.

in the d^2 Tanabe Sugano energy level diagram of Figure 1.[18] The absorption and luminescence properties of both systems have been studied in detail previously,[8,19,20] and therefore this paper focuses on their upconversion properties. In particular, we want to explore the influence of the identity of the first excited state on the upconversion mechanism and on the efficiency of the Ti^{2+} upconversion process.

II. Experimental Section

A. Crystal Growth. NaCl and $MgCl_2$ single crystals doped with Ti^{2+} (0.2%/0.8% and 0.1%) were grown from the melt by the Bridgeman technique. All of the handling of the starting materials and the resulting crystals was carried out under nitrogen. The actual dopant concentrations were estimated on the basis of published extinction values or absorption oscillator strengths.[8,21] The Ti^{2+} ions were generated in the melt by oxidation of Ti metal with $ZnCl_2$. The Zn metal produced in this reaction was deposited on the surfaces of the crystal in the Bridgeman ampule. Previous studies have shown that the Ti^{2+} dopant ion substitutes for Na^+ in NaCl,[19] and for Mg^{2+} in $MgCl_2$.[20] These studies have also demonstrated that the local symmetries of the Ti^{2+} dopant sites are very close to O_h in Ti^{2+}:NaCl and D_{3d} in the case of Ti^{2+}:$MgCl_2$. For simplicity we will use O_h term symbols throughout this paper unless otherwise stated.

B. Spectroscopic Measurements. For the spectroscopic measurements the samples were either enclosed in a copper cell or sealed in silica ampules, filled with He gas for heat dissipation. Sample cooling was achieved by a closed-cycle cryostat (Air Products Displex) for absorption measurements and with a He gas flow technique for the emission experiments.

Absorption spectra were measured on a Cary 5e (Varian) spectrometer. For continuous-wave (CW) luminescence spectroscopy the samples were excited with the 647.1 nm line of a Kr^+ laser (Coherent CR 550K) in the case of Ti^{2+}:NaCl, and with the 514.5 nm line of an Ar^+ laser (Ion Laser Technology) in the case of Ti^{2+}:$MgCl_2$. The sample luminescence was dispersed by a 0.75 m single monochromator (Spex 1702) equipped with 750/1250/1600 nm blazed (600 grooves/mm) gratings. $^3T_{1g}(t_{2g}e_g) \rightarrow {}^3T_{1g}(t_{2g}^2)$ emission was measured with a cooled photomultiplier tube (RCA C31034) and a photon-counting system (Stanford Research 400). $^3T_{2g}(t_{2g}e_g)/{}^1T_{2g}(t_{2g}^2) \rightarrow {}^3T_{1g}(t_{2g}^2)$ luminescence was measured with a liquid nitrogen cooled Ge detector (ADC 403L). Survey luminescence spectra were recorded with a dry ice cooled PbS detector (Hamamatsu P3337). The Ge- and PbS-detector signals were processed by a lock-in amplifier (Stanford Research 830).

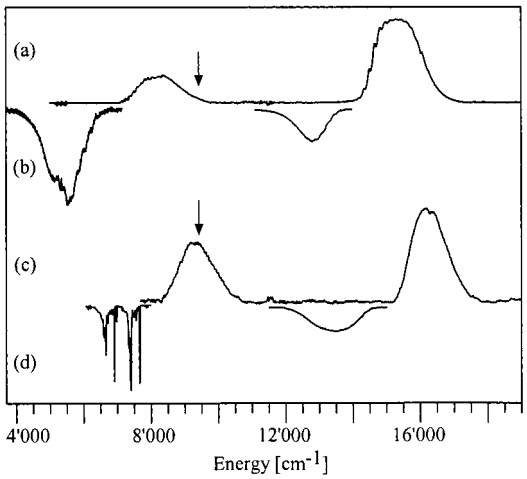

Figure 2. 15 K survey absorption spectra of (a) 0.8% Ti^{2+}:NaCl and (c) 0.1% Ti^{2+}:$MgCl_2$. The 15 K survey luminescence spectra of (b) 0.2% Ti^{2+}:NaCl and (d) 0.1% Ti^{2+}:$MgCl_2$ are displayed upside down. The arrows indicate the excitation energy used for the upconversion experiments in Figure 4.

For the upconversion luminescence and transient measurements the samples were excited with a pulsed Nd^{3+}:YAG laser (Quanta Ray DCR3, 1064 nm). The sample upconversion luminescence decay was detected as described above and recorded on a multichannel scaler (Stanford Research 430). For the upconversion excitation spectrum of Ti^{2+}:$MgCl_2$ and the measurements of the upconversion efficiencies an Ar^+ laser (Spectra Physics 2060-105A) pumped Ti:sapphire laser (Spectra Physics 3900S) was used.

For the measurement of the $^3T_{2g}(t_{2g}e_g)/{}^1T_{2g}(t_{2g}^2)$ lifetimes a fast-response Ge detector (ADC 403HS, response time 1 μs) connected to an oscilloscope (Tektronix TDS 540A) was used.

Using the procedure by Ejder,[22] all luminescence spectra were corrected for the sensitivity of the detection system and are displayed as photon counts versus energy.

III. Results

Figure 2 shows the 15 K survey absorption (traces a and c) and CW luminescence spectra (traces b and d) of 0.8% (a)/0.2% (b) Ti^{2+}:NaCl and of 0.1% Ti^{2+}:$MgCl_2$ (c, d). The luminescence spectra were obtained after excitation at 15454 cm^{-1} (b) and at 19436 cm^{-1} (d), respectively, and are displayed upside down. The visible and near-infrared luminescence transitions shown here were recorded with individual highly sensitive detection systems (see section II). The photon output ratio of visible:near-infrared luminescence is 1:4 in Ti^{2+}:NaCl and 2.1:1 in Ti^{2+}:$MgCl_2$, respectively. These ratios have been determined in separate luminescence experiments with a detection system which is sensitive in both spectral regions (see section II).

Figure 3 presents the 15 K decays of (a) $^3T_{2g}(t_{2g}e_g) \rightarrow {}^3T_{1g}(t_{2g}^2)$ luminescence in Ti^{2+}:NaCl and (b) $^1T_{2g}(t_{2g}^2) \rightarrow {}^3T_{1g}(t_{2g}^2)$ in Ti^{2+}:$MgCl_2$. Note that the *x*-scale is expanded in panel b compared to panel a by a factor of 100. The respective excited-state lifetimes extracted from these data are 1.4 ms for $^3T_{2g}(t_{2g}e_g)$ in Ti^{2+}:NaCl and 109 ms for $^1T_{2g}(t_{2g}^2)$ in Ti^{2+}:$MgCl_2$, see Table 1.

(18) Sugano, S.; Tanabe, Y.; Kamimura, H. *Multiplets of Transition Metal Ions in Crystals*; Academic Press: New York/London, 1970.
(19) Wenger, O. S.; Güdel, H. U. *J. Phys. Chem. B* **2001**, *105*, 4181−4187.
(20) Jacobsen, S. M.; Güdel, H. U.; Daul, C. A. *J. Am. Chem. Soc.* **1988**, *110*, 7610−7616.
(21) Brown, D. H.; Hunter, A.; Smith, W. E. *J. Chem. Soc., Dalton Trans.* **1979**, 79−82.
(22) Ejder, J. *Opt. Soc. Am.* **1969**, *59*, 223.

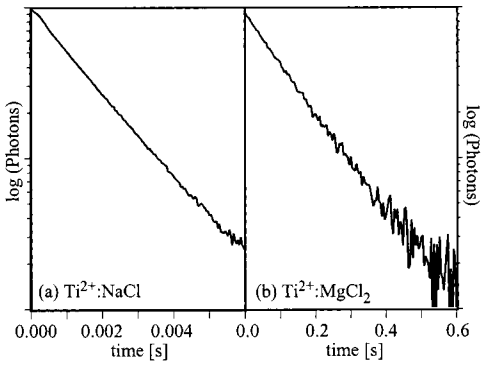

Figure 3. 15 K decay curves in semilog representation of (a) $^3T_{2g}(t_{2g}e_g) \rightarrow {}^3T_{1g}(t_{2g}^2)$ luminescence in Ti^{2+}:NaCl (detected at 6060 cm^{-1}) and (b) $^1T_{2g}(t_{2g}^2) \rightarrow {}^3T_{1g}(t_{2g}^2)$ luminescence in Ti^{2+}:$MgCl_2$ (detected at 7400 cm^{-1}). Excitation energies were 9500 and 9900 cm^{-1}, respectively.

Table 1. 15 K Lifetimes τ of the Metastable Excited States and Calculated 15 K $^3T_{1g}(t_{2g}e_g) \rightarrow {}^3T_{1g}(t_{2g}^2)$ Luminescence Quantum Yields η_{vis} in 0.2% Ti^{2+}:NaCl and 0.1% Ti^{2+}:$MgCl_2$, Respectively

	Ti^2:NaCl	Ti^{2+}:$MgCl_2$
$\tau(^3T_{2g}(t_{2g}e_g))$	1.4 ms	
$\tau(^1T_{2g}(t_{2g}^2))$		109 ms
$\tau(^3T_{1g}(t_{2g}e_g))$	15 μs	19 μs
$\eta_{vis}(^3T_{1g}(t_{2g}e_g) \rightarrow {}^3T_{1g}(t_{2g}^2))$	$\approx 0.26^a$	$\approx 0.7^b$

[a] From ref 19. [b] From ref 8.

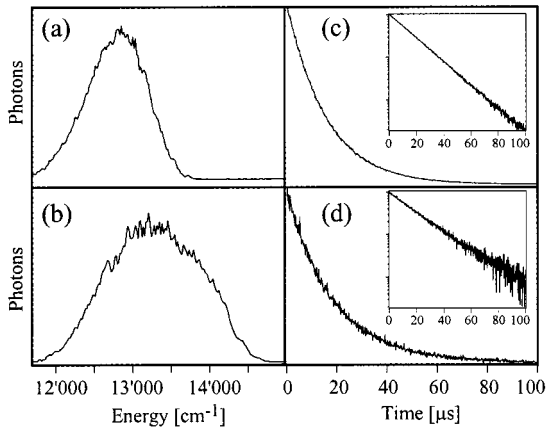

Figure 4. Left: 15 K $^3T_{1g}(t_{2g}e_g) \rightarrow {}^3T_{1g}(t_{2g}^2)$ upconversion luminescence spectra of (a) 0.2% Ti^{2+}:NaCl and (b) 0.1% Ti^{2+}:$MgCl_2$ obtained after pulsed excitation at 9399 cm^{-1}. Right: Upconversion luminescence dynamics of (c) 0.2% Ti^{2+}:NaCl and (d) 0.1% Ti^{2+}:$MgCl_2$ at 15 K following an 8 ns (9399 cm^{-1}) laser pulse. The insets show the same data in a semilogarithmic representation.

In the left part of Figure 4 the 15 K $^3T_{1g}(t_{2g}e_g) \rightarrow {}^3T_{1g}(t_{2g}^2)$ upconversion luminescence spectra of (a) 0.2% Ti^{2+}:NaCl and (b) 0.1%Ti^{2+}:$MgCl_2$ obtained after pulsed excitation at 9399 cm^{-1} are shown. The right part of Figure 4 shows the temporal evolution of the upconversion luminescence at 15 K after a 9399 cm^{-1} excitation pulse of 8 ns width in 0.2% Ti^{2+}:NaCl (c) and 0.1%Ti^{2+}:$MgCl_2$ (d). The insets show the same data in a semilogarithmic representation.

Figure 5a shows the excited-state excitation (ESE) spectrum of Ti^{2+}:$MgCl_2$ at 6 K (adapted from ref 8). In this experiment a (lamp) pump source provided a steady-state population in $^1T_{2g}(t_{2g}^2)$ by efficiently exciting into $^3T_{2g}(t_{2g}e_g)$. Luminescence from the $^3T_{1g}(t_{2g}e_g)$ higher excited state was monitored, while a (lamp) probe source was scanned through the $^1T_{2g}(t_{2g}^2) \rightarrow {}^1A_{1g}(t_{2g}^2)$/ $^1T_{2g}(t_{2g}e_g)$ excited-state absorption (ESA) transitions. Further experimental details are given in ref 8. Figure 5b presents the 15 K $^3T_{1g}(t_{2g}^2) \rightarrow {}^3T_{2g}(t_{2g}e_g)$ ground-state absorption (GSA) spectrum of Ti^{2+}:$MgCl_2$. Figure 5d shows the 15 K one-color excitation spectrum of $^3T_{1g}(t_{2g}e_g) \rightarrow {}^3T_{1g}(t_{2g}^2)$ upconversion luminescence in Ti^{2+}:$MgCl_2$.

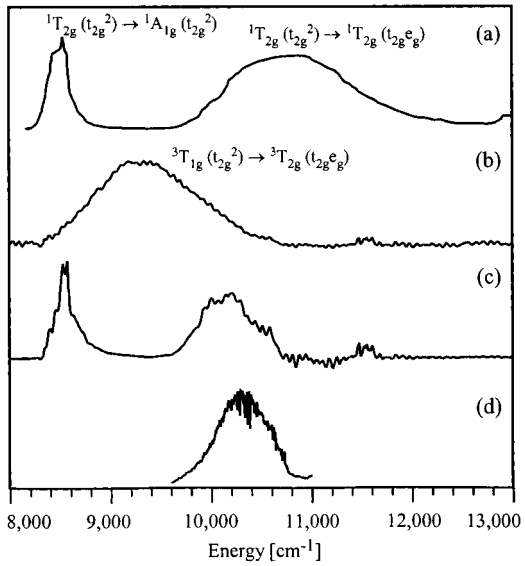

Figure 5. (a) Excited-state excitation (ESE) spectrum of Ti^{2+}:$MgCl_2$ at 6 K obtained after two-color upconversion excitation, the first color exciting the $^3T_{2g}(t_{2g}e_g)$ absorption around 9300 cm^{-1}. Adapted from ref 8. (b) 15 K $^3T_{1g}(t_{2g}^2) \rightarrow {}^3T_{2g}(t_{2g}e_g)$ ground-state absorption (GSA) spectrum of 0.1% Ti^{2+}:$MgCl_2$. (c) Calculated product of the ESE and GSA spectra from traces a and b. (d) Experimental 15 K one-color upconversion excitation spectrum of Ti^{2+}:$MgCl_2$ obtained after detection at 13400 cm^{-1}.

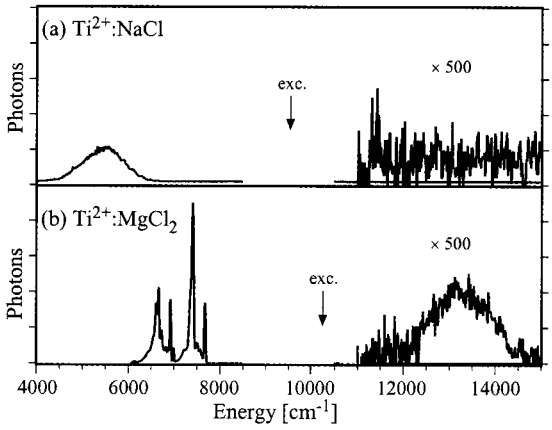

Figure 6. 15 K survey luminescence spectra obtained after near-infrared excitation in (a) 0.2% Ti^{2+}:NaCl and (b) 0.1% Ti^{2+}:$MgCl_2$. Excitation occurred at 9500 cm^{-1} (a) and 10300 cm^{-1} (b), respectively (see arrows), with identical excitation densities (see section III). Both spectra are normalized to an equal integrated near-infrared luminescence intensity. The spectral regions between 11000 and 15000 cm^{-1} are shown on a 500 times enlarged *y*-scale.

Figure 6 shows the 15 K survey luminescence spectra of (a) Ti^{2+}:NaCl and (b) Ti^{2+}:$MgCl_2$ obtained after excitation at 9500 and 10300 cm^{-1}, respectively, see arrows. For both experiments an excitation power of 40 mW and a focusing lens with $f = 5$ cm was used. Both spectra are normalized to an equal integrated near-infrared luminescence intensity. The 11000−15000 cm^{-1} spectral regions of $^3T_{1g}(t_{2g}e_g) \rightarrow {}^3T_{1g}(t_{2g}^2)$ upconversion luminescence are shown on a 500 times enlarged scale. This vis: NIR luminescence intensity ratio is about 1:100 for Ti^{2+}:$MgCl_2$ and below 1:1000 for Ti^{2+}:NaCl under these conditions.

IV. Analysis and Discussion

A. Energy Level Sequence in Ti^{2+}:NaCl and Ti^{2+}:$MgCl_2$. The 15 K survey absorption spectra of 0.8% Ti^{2+}:NaCl and 0.1% Ti^{2+}:$MgCl_2$ presented in Figure 2 show the typical features of octahedrally coordinated d^2 ions.[23] Two intense broad bands are observed in both spectra, and according to the d^2 Tanabe Sugano energy level diagram (Figure 1) they are assigned to the spin-allowed one-electron transitions from the $^3T_{1g}(t_{2g}^2)$ ground state to the $^3T_{2g}(t_{2g}e_g)$ and $^3T_{1g}(t_{2g}e_g)$ excited states. Spin forbidden triplet−singlet transitions are not observed in the absorption spectra, and this is due to the strictness of the spin selection rule in Ti^{2+}, caused by the low spin−orbit coupling in this ion: The free Ti^{2+} ion spin−orbit coupling parameter ζ is 123 cm^{-1},[24] and in Ti^{2+}:$MgCl_2$ it was found to be reduced to 93 cm^{-1}.[20] For Ti^{2+}:$MgCl_2$ a ligand field calculation was carried out earlier.[20] A fit of calculated to experimental excited-state energies yielded the octahedral ligand field parameters 10 Dq = 10180 cm^{-1}, B = 527 cm^{-1}, and C/B = 3.76 for this system. We carried out an analogous fit for Ti^{2+}:NaCl using the same C/B ratio and obtained 10 Dq = 9064 $cm^{-1}$and B = 530 cm^{-1}. The large difference of roughly 1100 cm^{-1} between 10 Dq values in Ti^{2+}:$MgCl_2$ and Ti^{2+}:NaCl can be rationalized by a simple comparison of ionic radii: Ti^{2+} is smaller than Na^+ (1.00 vs 1.16 Å), but it is larger than Mg^{2+} (1.00 vs 0.86 Å). Consequently, the Ti^{2+} dopant ion experiences a much stronger ligand field in $MgCl_2$ than in NaCl. Thus one calculates a (10 Dq):B ratio of 17.1 for Ti^{2+}:NaCl and 19.3 for Ti^{2+}:$MgCl_2$. This places the Ti^{2+}:NaCl system a little to the left of the $^3T_{2g}(t_{2g}e_g)$/$^1T_{2g}(t_{2g}^2)$ crossing point in the d^2 Tanabe Sugano diagram, whereas Ti^{2+}:$MgCl_2$ is located to the right of this crossing point, and this is illustrated by the dashed vertical lines in Figure 1. It should be noted that the assumption of a strictly octahedral ligand field is a very crude approximation for Ti^{2+}:$MgCl_2$, since in this lattice the Ti^{2+} dopant ion is located in a site of trigonal symmetry,[20] and it has been demonstrated previously that in this system the effect of the trigonal field on the Ti^{2+} ground- and excited-state splittings is on the order of several hundred wavenumbers.[25,20]

B. Identification of the Emitting States in Ti^{2+}:NaCl and Ti^{2+}:$MgCl_2$. The 15 K survey luminescence spectra of 0.2% Ti^{2+}:NaCl and 0.1% Ti^{2+}:$MgCl_2$ are displayed upside down in Figure 2, and these spectra were obtained after excitation into $^3T_{1g}(t_{2g}e_g)$ at 15454 cm^{-1} in the case of Ti^{2+}:NaCl (b) and after $^3A_{2g}(e_g^2)$ excitation at 19436 cm^{-1} in Ti^{2+}:$MgCl_2$. Both spectra consist of two emission bands. The higher energy emission bands are centered around 12800 cm^{-1} in Ti^{2+}:NaCl and around 13300 cm^{-1} in Ti^{2+}:$MgCl_2$. On the basis of their energetic positions and their band shapes they are assigned to the $^3T_{1g}(t_{2g}e_g) \rightarrow {}^3T_{1g}(t_{2g}^2)$ transitions. There is a remarkable difference between the widths of the respective luminescence bands in Ti^{2+}:NaCl and Ti^{2+}:$MgCl_2$, respectively. The full width at half-maximum is roughly 900 cm^{-1} in the former, whereas in the latter it is approximately 1600 cm^{-1}. This is attributed to the large trigonal splitting of the $^3T_{1g}(t_{2g}^2)$ ground state in Ti^{2+}:$MgCl_2$. Previous studies have revealed that this splitting is on the order of 700 cm^{-1}.[20,25]

In the lower energy luminescence bands there are significant and very important differences between Ti^{2+}:NaCl and Ti^{2+}:$MgCl_2$. In both systems these luminescence bands have a very different decay behavior than the $^3T_{1g}(t_{2g}e_g) \rightarrow {}^3T_{1g}(t_{2g}^2)$ luminescence bands (see section IV.C), and consequently they are due to emission from some excited state other than $^3T_{1g}(t_{2g}e_g)$. In Ti^{2+}:NaCl the 15 K near-infrared luminescence band consists of a single broad band centered around 5400 cm^{-1} (trace b in Figure 2). According to its band shape and its energetic position, it is assigned to the $^3T_{2g}(t_{2g}e_g) \rightarrow {}^3T_{1g}(t_{2g}^2)$ transition, in agreement with our conclusion from section IV.A, namely, that $^3T_{2g}(t_{2g}e_g)$ is the first excited state in Ti^{2+}:NaCl (see Figure 1). In Ti^{2+}:$MgCl_2$, on the other hand, 15 K near-infrared luminescence occurs as a series of sharp lines (trace d in Figure 2), indicating that ground and emitting state are hardly displaced relative to each other. This is typically the case between states which derive from the same electron configuration, and therefore this near-infrared luminescence has been assigned to the $^1T_{2g}(t_{2g}^2) \rightarrow {}^3T_{1g}(t_{2g}^2)$ transition.[20] A component of $^1T_{2g}(t_{2g}^2)$ is thus the first excited state in Ti^{2+}:$MgCl_2$.

Finally, we briefly note that in Ti^{2+}:$MgCl_2$ at 7 K weak $^3T_{1g}(t_{2g}e_g) \rightarrow {}^3T_{2g}(t_{2g}e_g)$ inter-excited-state luminescence around 6200 cm^{-1}has been observed.[8] This emission is roughly a factor of 50 less intense than the $^3T_{1g}(t_{2g}e_g) \rightarrow {}^3T_{1g}(t_{2g}^2)$ emission. In Ti^{2+}:NaCl the respective inter-excited-state luminescence was too weak to be observed.[19] In summary, at 15 K dual luminescence is observed in both Ti^{2+}:NaCl and Ti^{2+}:$MgCl_2$, and thus both systems fulfill the basic condition for photon upconversion processes. However, the identity of the first excited state is different in these two systems and, as we shall see in the following sections, this has a major impact on their upconversion properties.

C. Excited-State Dynamics and Temperature-Dependent Emission Properties. In this section we shall briefly discuss the differences in the excited-state dynamics of Ti^{2+}:NaCl and Ti^{2+}:$MgCl_2$, respectively, since this will be relevant for the discussion of their different upconversion properties in sections IV.D/E. First, we discuss the different dynamics of the respective lowest excited states in Ti^{2+}:NaCl and Ti^{2+}:$MgCl_2$, respectively. At 15 K, the $^3T_{2g}(t_{2g}e_g)$ lifetime in 0.2% Ti^{2+}:NaCl is 1.4 ms, whereas the $^1T_{2g}(t_{2g}^2)$ lifetime in 0.1% Ti^{2+}:$MgCl_2$ is 109 ms, see Figure 3 and Table 1. This large difference is explained as follows: In both systems the depopulation of the lowest excited state occurs entirely radiatively at temperatures below 150 K,[19,20] and therefore it is due to a difference in the respective *radiative* lifetimes. The radiative lifetime of an excited state $|b\rangle$ is inversely proportional to the oscillator strength of an absorption transition $|a\rangle \rightarrow |b\rangle$.[26] The relevant oscillator strengths for our consideration here are those of the spin-allowed $^3T_{1g}(t_{2g}^2) \rightarrow {}^3T_{2g}(t_{2g}e_g)$ and the spin-forbidden $^3T_{1g}(t_{2g}^2) \rightarrow {}^1T_{2g}(t_{2g}^2)$ absorption transitions for Ti^{2+}:NaCl and Ti^{2+}:$MgCl_2$, respectively. The difference between these oscillator strengths is responsible for the large difference between the $^3T_{2g}(t_{2g}e_g)$ (Ti^{2+}:NaCl) and $^1T_{2g}(t_{2g}^2)$ (Ti^{2+}:$MgCl_2$) lifetimes at 15 K.

The 15 K lifetime of the $^3T_{1g}(t_{2g}e_g)$ higher excited state is almost identical in both systems considered here: As shown in Table 1 it is 15 μs in 0.2% Ti^{2+}:NaCl and 19 μs in 0.1% Ti^{2+}:$MgCl_2$. In both cases, $^3T_{1g}(t_{2g}e_g)$ depopulation has been demonstrated to occur to a significant extent via nonradiative multiphonon relaxation already at the lowest temperatures. As discussed in section IV.B, $^3T_{1g}(t_{2g}e_g)$ luminescence to lower lying excited states is negligible, and therefore the $^3T_{1g}(t_{2g}e_g) \rightarrow {}^3T_{1g}(t_{2g}^2)$ luminescence quantum yield η_{vis} is a good measure

(23) Reber, C.; Güdel, H. U. *J. Lumin.* **1988**, *42*, 1−13 and references therein.
(24) Figgis, B. *Introduction to Ligand Fields*; Interscience: New York, 1966; p 60.
(25) Jacobsen, S. M.; Smith, W. E.; Reber, C.; Güdel, H. U. *J. Chem. Phys*. **1986**, *84*, 5205−5206.
(26) Brunold, T. C.; Güdel, H. U. In *Inorganic Electronic Structure and Spectroscopy*; Solomon, E. I., Lever, A. B. P., Eds.; Wiley: New York, 1999; pp 259−306.

to quantify these nonradiative multiphonon relaxation processes. The 15 K values of η_{vis} for the two systems considered here are given in Table 1. These quantum yields were calculated in refs 8 and 19 on the basis of lifetime data and emission intensity ratios. Table 1 shows that there is a significant difference between η_{vis} in the two systems considered here: In Ti^{2+}:NaCl it is around 0.26, whereas in Ti^{2+}:$MgCl_2$ a value of approximately 0.7 was found.

At elevated temperatures, i.e., above 40 K in 0.1% Ti^{2+}:$MgCl_2$ and above 100 K in 0.2% Ti^{2+}:NaCl, multiphonon relaxation quenches the $^3T_{1g}(t_{2g}e_g)$ emission completely, and thus the upconversion experiments discussed in the following sections were performed at 15 K.

D. Upconversion Mechanisms. As shown in the left part of Figure 4, at 15 K excitation of 0.2% Ti^{2+}:NaCl and 0.1% Ti^{2+}:$MgCl_2$ at 9399 cm^{-1} leads to luminescence at higher energies. From a comparison with the emission data in Figure 2 (traces b and d), the assignment of the upconversion luminescence bands in Figure 4 to the $^3T_{1g}(t_{2g}e_g) \rightarrow {}^3T_{1g}(t_{2g}^2)$ transition is straightforward. The spectra shown in Figure 4 represent the first observation of Ti^{2+} upconversion luminescence after excitation at a single wavelength, i.e., so-called one-color excitation. Very often the temporal behavior of the upconversion luminescence after a short excitation pulse is used to distinguish between potential upconversion mechanisms.[27] In the right part of Figure 4 the temporal evolution of the 15 K upconversion luminescence in (c) 0.2% Ti^{2+}:NaCl and (d) 0.1% Ti^{2+}:$MgCl_2$ after an 8 ns (9399 cm^{-1}) excitation pulse is shown. Very similar upconversion transients are observed in the two systems: an instantaneous single-exponential decay (see the straight lines in the insets of Figure 4). The decay times are 15 and 19 μs in 0.2% Ti^{2+}:NaCl and 0.1% Ti^{2+}:$MgCl_2$, respectively, and thus correspond to the 15 K $^3T_{1g}(t_{2g}e_g)$ lifetimes after direct $^3T_{1g}(t_{2g}e_g)$ excitation, see Table 1. The fact that the $^3T_{1g}(t_{2g}e_g)$ population decays instantaneously after the excitation pulse indicates that the whole upconversion process takes place within the 8 ns duration of the laser pulse. We conclude that the involved upconversion steps are radiative. Nonradiative upconversion steps would, since they can proceed after the laser pulse, typically lead to a rise preceding the decay.[13,27] The upconversion transients of Figure 4 are thus typical for a sequence of ground-state absorption (GSA) and excited-state absorption (ESA) steps.[28]

We now turn to an identification of the relevant GSA and ESA transitions in Ti^{2+}:NaCl and Ti^{2+}:$MgCl_2$. In section IV.A we have shown that efficient GSA in Ti^{2+}-doped systems can only occur on spin-allowed triplet−triplet transitions. Consequently, the upconversion relevant GSA transition is $^3T_{1g}(t_{2g}^2) \rightarrow {}^3T_{2g}(t_{2g}e_g)$ in both systems considered here. The 9399 cm^{-1} excitation source, in particular, hits into the high-energy tail and into the band maximum of the respective 15 K absorption bands in Ti^{2+}:NaCl and Ti^{2+}:$MgCl_2$, respectively, see the arrows in Figure 2.

For Ti^{2+}:$MgCl_2$ the upconversion relevant ESA transitions can be identified on the basis of the 15 K excited-state excitation (ESE) spectrum presented in Figure 5a. It consists of a relatively narrow band centered at about 8500 cm^{-1} and a broader band centered around 10800 cm^{-1}. The initial state of these ESA transitions is the metastable intermediate state $^1T_{2g}(t_{2g}^2)$, and we assign the bands to singlet−singlet transitions (see section IV.A). According to the d^2 Tanabe Sugano diagram in Figure 1 and their band shapes, the two features in Figure 5a are assigned as follows: The band at about 8500 cm^{-1} is due to the *intraconfigurational* $^1T_{2g}(t_{2g}^2) \rightarrow {}^1A_{1g}(t_{2g}^2)$ transition, in agreement with its narrow bandwidth. The band around 10800 cm^{-1} corresponds to the *interconfigurational* $^1T_{2g}(t_{2g}^2) \rightarrow {}^1T_{2g}(t_{2g}e_g)$ transition and is therefore much broader.[8] Figure 5c shows the calculated product of these ESA (5a) and GSA (5b) spectra. The one-color upconversion excitation spectrum obtained in the 9600−11000 cm^{-1} spectral range is displayed in Figure 5d, and this spectrum compares very favorably to the calculated trace in Figure 5c. This indicates that in 0.1% Ti^{2+}:$MgCl_2$ a GSA/ESA upconversion mechanism is active for excitation in the whole spectral range between 9600 and 11000 cm^{-1}. Furthermore these data show that the most efficient upconversion for one-color excitation occurs with an excitation energy of about 10300 cm^{-1}. Figure 5c indicates that an excitation energy of about 8540 cm^{-1} is expected to lead to an even higher upconversion efficiency. However, this excitation energy is far below the Ti^{3+}:sapphire laser tuning range, and we are not able to test this experimentally. Nevertheless, the coincidence of Figures 5c and 5d between 9600 and 11000 cm^{-1} is convincing evidence for a GSA/ESA upconversion mechanism. Finally, we note that an excitation energy of 9399 cm^{-1} as used for the upconversion transient measurements (Figure 4) constitutes a very inefficient upconversion excitation scheme for Ti^{2+}:$MgCl_2$: From Figure 5c we calculate that at this energy the GSA/ESA product is approximately a factor of 80 lower than at 10300 cm^{-1}.

For Ti^{2+}:NaCl no ESE spectrum is available, and we will discuss in section IV.E why such an experiment is far more difficult to perform in Ti^{2+}:NaCl than in Ti^{2+}:$MgCl_2$. Even without an ESE spectrum, the identification of the upconversion relevant ESA transition in Ti^{2+}:NaCl is straightforward according to simple energy considerations and the spin selection rule: In this system ESA transitions originate from $^3T_{2g}(t_{2g}e_g)$ and most likely lead to final triplet states. From the 15 K survey GSA spectrum of Ti^{2+}:NaCl we estimate that $^3T_{2g}(t_{2g}e_g) \rightarrow {}^3T_{1g}(t_{2g}e_g)$ ESA occurs around 7000 cm^{-1}, and since this is an *intraconfigurational* transition, a relatively sharp band is expected. Figure 7a presents a single configurational coordinate (SCC) diagram for Ti^{2+}:NaCl. This SCC picture was plotted on the basis of the absorption spectrum in Figure 2 and a d^2 ligand field calculation.[19,29] From this SCC model the $^3T_{2g}(t_{2g}e_g)$

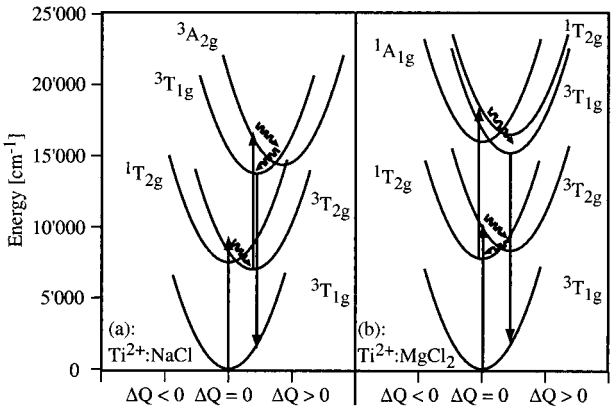

Figure 7. Single configurational coordinate (SCC) representation of the relevant excited states in Ti^{2+}:NaCl (left) and Ti^{2+}:$MgCl_2$ (right). The solid upward and downward arrows represent absorption and luminescence transitions, respectively, and wavy arrows indicate nonradiative relaxation processes.

(27) Gamelin, D. R.; Güdel, H. U. *Acc. Chem. Res.* **2000**, *33*, 235−242.
(28) Krämer, K. W.; Güdel, U. U.; Schwartz, R. N. *J. Alloys Compd.* **1998**, *275*−*277*, 191−195.
(29) Liehr, A. D.; Ballhausen, C. J. *Ann. Phys.* **1959**, *2*, 134−155.

$\rightarrow {}^3A_{2g}(e_g^2)$ ESA band maximum is estimated to occur at about 10000 cm^{-1}. For this interconfigurational transition a broad band with a width on the order of 1000 cm^{-1} is expected. Thus, there is a significant spectral overlap between this latter ESA transition and the ${}^3T_{1g}(t_{2g}^2) \rightarrow {}^3T_{2g}(t_{2g}e_g)$ GSA at 9399 cm^{-1}.

Figure 7 summarizes the results from this section in a single configurational coordinate (SCC) picture for Ti^{2+}:NaCl (left) and Ti^{2+}:$MgCl_2$ (right). The SCC diagram of the latter was adapted from ref 8. In Ti^{2+}:NaCl upconversion after excitation at 9399 cm^{-1} occurs via ${}^3T_{1g}(t_{2g}^2) \rightarrow {}^3T_{2g}(t_{2g}e_g)$ GSA and ${}^3T_{2g}(t_{2g}e_g) \rightarrow {}^3A_{2g}(e_g^2)$ ESA, i.e., two triplet−triplet transitions, which both involve an electron promotion from a t_{2g} to an e_g orbital. This is followed by nonradiative relaxation to the ${}^3T_{1g}(t_{2g}e_g)$ state, from which luminescence occurs. In Ti^{2+}:$MgCl_2$ ${}^3T_{1g}(t_{2g}^2) \rightarrow {}^3T_{2g}(t_{2g}e_g)$ GSA is followed by nonradiative relaxation to the metastable ${}^1T_{2g}(t_{2g}^2)$ state. From there, ESA at 9399 cm^{-1} occurs into weak ${}^1A_{1g}(t_{2g}^2)$ phonon sidebands (see Figure 5a), and this corresponds to an *intraconfigurational* singlet−singlet transition. This is followed by nonradiative relaxation to the emitting ${}^3T_{1g}(t_{2g}e_g)$ state.

Finally, we briefly comment on the possibility of energy transfer upconversion (ETU) contributions to the upconversion process in Ti^{2+}:NaCl and Ti^{2+}:$MgCl_2$, respectively, after excitation energies different from 9399 cm^{-1}. In an ETU process two ions excited to the intermediate level by GSA undergo a nonradiative energy transfer process in which one ion ends up in the upper excited state and the other one in the ground state. Simply from the fact that after excitation at 9399 cm^{-1} upconversion occurs by a pure GSA/ESA mechanism (Figure 4), we cannot a priori exclude such ETU contributions for other excitation energies. However, we can exclude them on the basis of simple spectral overlap arguments: For an energy transfer process to occur, a nonzero spectral overlap between a donor emission and an acceptor absorption profile is required.[26,30] In the specific case of ETU in Ti^{2+}:$MgCl_2$ the relevant profiles are those of the ${}^1T_{2g}(t_{2g}^2) \rightarrow {}^3T_{1g}(t_{2g}^2)$ emission (trace d in Figure 2) and ${}^1T_{2g}(t_{2g}^2) \rightarrow {}^1A_{1g}(t_{2g}^2)/{}^1T_{2g}(t_{2g}e_g)$ excited state absorption (trace a in Figure 5). Comparison of theses traces shows that at 15 K this overlap is essentially zero, and thus no resonant ETU can occur in Ti^{2+}:$MgCl_2$ at this temperature. So-called phonon-assisted ETU can also be excluded for Ti^{2+}:$MgCl_2$ at this temperature, because it is an endothermic process. In Ti^{2+}:NaCl, on the other hand, the relevant transitions are ${}^3T_{2g}(t_{2g}e_g) \rightarrow {}^3T_{1g}(t_{2g}^2)$ emission (trace b in Figure 2) and ${}^3T_{2g}(t_{2g}e_g) \rightarrow {}^3T_{1g}(t_{2g}e_g)$ (excited state) absorption (no available experimental data, see above). At 15 K this emission extends from approximately 6700 cm^{-1} to lower energies, whereas the relevant sharp ESA transition is calculated to occur at about 7000 cm^{-1} (see above). Again, ETU at 15 K can be ruled out for energetic reasons.

E. Comparison of the Upconversion Efficiencies in Ti^{2+}:NaCl and Ti^{2+}:$MgCl_2$. Our aim in this section is a general discussion of the relative upconversion efficiencies in Ti^{2+}:NaCl and Ti^{2+}:$MgCl_2$, respectively, and it will therefore not be restricted to a one-color 9399 cm^{-1} excitation scheme. Rather we calculate and compare the efficiencies for a so-called two-color upconversion excitation scheme, in which one laser is in resonance with the GSA maximum and a second laser is in resonance with the ESA maximum. The upconversion efficiency is defined as the ratio of visible photon output versus near-infrared photon input. Figure 8 shows the relevant upconversion steps in Ti^{2+}:NaCl (left) and Ti^{2+}:$MgCl_2$ (right), respectively, in a simple energy level diagram. The ${}^3T_{1g}(t_{2g}^2)$ ground state,

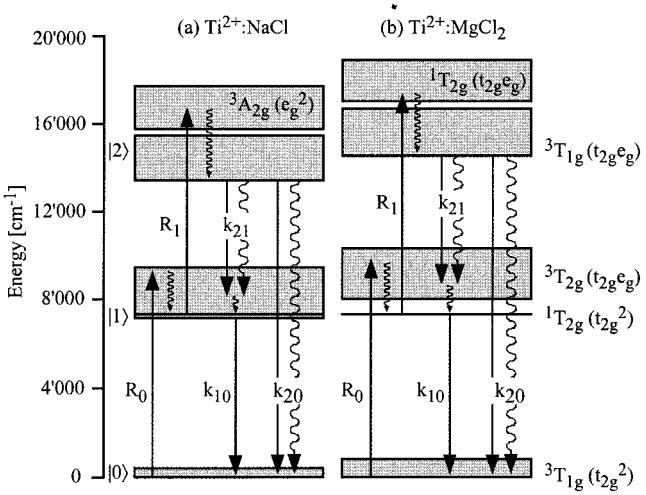

Figure 8. Schematic representation of the upconversion processes (upward arrows) and the possible relaxation pathways (downward arrows) in Ti^2:NaCl (a) and Ti^{2+}:$MgCl_2$ (b). Solid arrows denote the radiative processes of GSA, ESA, and luminescence, and wavy arrows indicate nonradiative multiphonon relaxation processes.

the ${}^3T_{2g}(t_{2g}e_g)/{}^1T_{2g}(t_{2g}^2)$ intermediate states, and the ${}^3T_{1g}(t_{2g}e_g)$ upper emitting state are denoted $|0\rangle$, $|1\rangle$, and $|2\rangle$, respectively. The following mathematical treatment exclusively deals with these three levels, i.e., nonradiative relaxation processes to the vibrational ground levels of the various metastable states (short wavy arrows) are considered to occur instantaneously. This is a very sound approximation since these processes typically occur on a picosecond time scale, whereas the 15 K lifetimes of the metastable electronic states in our systems are on the order of micro- and milliseconds, see Table 1.

The GSA ($i = 0$) and ESA ($i = 1$) transitions are represented by the straight upward arrows in Figure 8, and the rates R_i of these processes are given by

$$R_i = cP\sigma_i N_i \tag{1}$$

where c is a constant, P the laser power, and N_i the population density of level $|i\rangle$. σ_i is the absorption cross section at the laser excitation wavelength. The differential rate equation for the population density N_1 of the intermediate upconversion level is

$$\frac{dN_1}{dt} = R_0 - R_1 - k_{10}N_1 + k_{21}N_2 \tag{2}$$

where the first two terms represent ${}^3T_{2g}(t_{2g}e_g)/{}^1T_{2g}(t_{2g}^2)$ population by GSA and depopulation by ESA, respectively. The third term represents radiative decay of the level $|1\rangle$ population to the ground state with the decay rate constant k_{10}. In the last term all processes that repopulate ${}^3T_{2g}(t_{2g}e_g)/{}^1T_{2g}(t_{2g}^2)$ from the ${}^3T_{1g}(t_{2g}e_g)$ higher excited state with a total rate constant $k_{21}$are summarized. These processes are partly radiative and partly nonradiative,[8,19] as emphasized by the straight and curly downward arrows, respectively, in Figure 8. In the low-power limit R_1 is small, and consequently the population density N_2 is negligible. Under steady-state conditions N_1 is then

$$N_1 = R_0/k_{10} \tag{3}$$

Substitution of this expression in eq 1 leads to the following rate R_1 with which the upper emitting ${}^3T_{1g}(t_{2g}e_g)$ level ($|2\rangle$) is populated:[31]

(30) Henderson, B.; Imbusch, G. F. *Optical Spectroscopy of Inorganic Solids*; Oxford Science Publications: Oxford, 1989.

$$R_1 = c^2 P^2 N_0 \frac{\sigma_0 \sigma_1}{k_{10}} \quad (4)$$

R_1 is the upconversion rate we are interested in. The first three factors in eq 4 can be considered as identical for the two Ti^{2+} systems considered here. In both cases the GSA step corresponds to the $^3T_{1g}(t_{2g}^2) \rightarrow {}^3T_{2g}(t_{2g}e_g)$ transition, and consequently σ_0 is very similar in both systems. We have no direct information on the relative magnitudes of the ESA cross sections σ_1 in these two systems. On the basis of the fact that the upconversion relevant ESA transitions are spin-allowed in both systems, we assume that they are of comparable magnitude. The most important difference between Ti^{2+}:NaCl and Ti^{2+}:$MgCl_2$ lies in their different k_{10} values. These correspond to the inverse of the $^3T_{2g}(t_{2g}e_g)$ lifetime in Ti^{2+}:NaCl and the $^1T_{2g}(t_{2g}^2)$ lifetime in Ti^{2+}:$MgCl_2$, respectively. From Table 1 we obtain $k_{10} = 714$ s^{-1} for the former and $k_{10} = 9.2$ s^{-1} for the latter. On the basis of these numbers and eq 4, we calculate an upconversion rate R_1 which is about a factor of 80 larger for Ti^{2+}:$MgCl_2$ than for Ti^{2+}:NaCl. Consequently, we estimate that, after two-color excitation with one laser in resonance with the GSA maximum and a second laser in resonance with the ESA maximum, the achievable $^3T_{1g}(t_{2g}e_g)$ steady state population is roughly 80 times bigger in Ti^{2+}:$MgCl_2$ than in Ti^{2+}:NaCl. Taking their 15 K $^3T_{1g}(t_{2g}e_g) \rightarrow {}^3T_{1g}(t_{2g}^2)$ luminescence quantum yields into account (Table 1), this difference will be amplified: We calculate an efficiency of the upconversion process which is roughly 200 times higher for Ti^{2+}:$MgCl_2$ than for Ti^{2+}:NaCl at this temperature. In practice, however, this experiment is difficult to perform, mainly due to the lack of strong laser excitation sources in the 8000−9500 cm^{-1} spectral region. This is particularly the case for Ti^{2+}:NaCl where the upconversion relevant GSA and ESA transitions lie energetically below the Ti^{3+}:sapphire laser tunability range. Figure 6 presents 15 K survey luminescence spectra obtained after monochromatic near-infrared excitation in (a) 0.2% Ti^{2+}:NaCl and (b) 0.1% Ti^{2+}:$MgCl_2$. For both spectra identical excitation densities were used (see section III). Both spectra are normalized to an equal integrated near-infrared luminescence intensity. In the case of Ti^{2+}:$MgCl_2$(Figure 6b) the excitation energy was 10300 cm^{-1} (see arrow), i.e., the energy at which the GSA/ESA overlap is maximal, see Figure 5d. In this experiment the ratio of visible $^3T_{1g}(t_{2g}e_g) \rightarrow {}^3T_{1g}(t_{2g}^2)$ upconversion luminescence to near-infrared $^1T_{2g}(t_{2g}^2) \rightarrow {}^3T_{1g}(t_{2g}^2)$ luminescence is approximately 1:100. In the case of Ti^{2+}:NaCl an excitation energy of 9500 cm^{-1} was used, and as estimated from Figure 6a, this results in a visible (upconversion): NIR luminescence intensity ratio below 1:1000. This is consistent with our conclusion that the upconversion efficiency is higher in Ti^{2+}:$MgCl_2$ than in Ti^{2+}:NaCl. However, we note that 9500 cm^{-1} is very unlikely the energy at which the GSA/ESA overlap is maximal in Ti^{2+}:NaCl. The GSA maximum is around 8200 cm^{-1}, and the upconversion relevant ESA has been estimated to peak around 10000 cm^{-1} (see section IV.D), and thus excitation around 9000 cm^{-1} would more likely be optimal. This experiment, however, could not be performed to due the lack of a tunable laser source in this spectral region.

V. Conclusions

We have shown that photon upconversion in two chemically similar systems can occur by different mechanisms with very different efficiencies. The key factor here is the spin. In contrast to rare-earth ions spin is a very good quantum number in Ti^{2+}, and the spin selection rule is important. Similar to the situation in Cr^{3+} (d^3) systems, we have in Ti^{2+} (d^2) a spin-crossover situation in the first metastable excited state. At low crystal fields this metastable state $^3T_{2g}(t_{2g}e_g)$ has the same spin as the ground state, and above the crossing point $^1T_{2g}(t_{2g}^2)$ is the metastable state. Our two systems, Ti^{2+}:NaCl and Ti^{2+}:$MgCl_2$, have been chosen to lie below and above this excited state spin-crossover point, respectively. Our paper nicely illustrates how strongly the excited-state dynamics and the competition between the various radiative and nonradiative processes are affected by this crossover. In principle, we thus have a handle, which is nonexistent in rare-earth systems, to tune the excited-state dynamics and thus the upconversion behavior. This handle is based on the susceptibility of ligand field states of transition metal ions on small chemical and structural changes in the coordination sphere. In practice, on the other hand, we realize that neither Ti^{2+}:NaCl nor Ti^{2+}:$MgCl_2$ is a likely candidate for near-infrared to visible upconversion materials.

Acknowledgment. This work was financially supported by the Swiss National Science Foundation.

IC010255T

(31) Gamelin, D. R.; Güdel, H. U. In *Topics in Current Chemistry*; Yersin, H., Ed.; Springer-Verlag: Berlin, 2001; Vol. 214.